Efficiency Assessment of Air-Cooling System as a Final Heat Sink of the ATOM System

Doyoung Shin [a], Min Wook Na [a], Gwang Hyeok Seo [a], Yonghee Kim [b], Jeong Ik Lee [b], Sung Joong Kim [a, c*]
[a]*Department of Nuclear Engineering, Hanyang Univ.*
222 Wangsimni-ro, Seongdong-gu, Seoul 04763, Republic of Korea
[b]*Department of Nuclear and Quantum Engineering, Korea Advanced Institute of Science and Technology*
291 Daehak-ro, Yuseong-gu, Daejeon 34141, Republic of Korea
[c]*Institute of Nano Science & Technology, Hanyang Univ.*
222 Wangsimni-ro, Seongdong-gu, Seoul 04763, Republic of Korea
[*]*Corresponding author: sungjkim@hanyang.ac.kr*

1. Introduction

Recently, considerable attentions have been focused on Small Modular Reactors (SMRs) for its potential advantages, i.e. flexible siting, lower capital cost, or advanced safety characteristics [1]. In Korea, a new research project was started for the development of a further improved SMR that pursues inherent safety and autonomous operation, Autonomous Transportable On-demand reactor Module (ATOM). The project focuses on the boron-free primary coolant system and the air-cooled supercritical CO_2 (SCO_2) power conversion cycle [2]. These features allow the system to automatically load follow and response well to extreme environment conditions like desert with lack of cooling water [3].

The air-cooling system has been frequently utilized in many engineering plants worldwide. Two well-known types of air-cooling system exist. First is an Air-Cooled Condenser (ACC) which vapor enters the system and condenses as it passes through the pipe. Latent heat is removed by a mechanically generated air flow. Efficiency of the ACC system can be enhanced by mist evaporation outside the tube [4]. Second is a cooling tower with an intermediate loop of coolant to remove latent heat from the vapor and use naturally or mechanically occurred air flow to cool down the hot coolant. As the goal of the ATOM system is inherent safety, ACC is considered inappropriate due to a possibility of radioactive contamination if any pipe rupture occurs. Thus, the cooling tower air-cooling system is currently considered as a final heat sink of the ATOM system.

The objective of this study is to assess the heat removal efficiency of the air-cooling system as a final heat sink. As a 1st phase of the ATOM development, we first consider the water/steam as a working fluid rather than SCO_2. Overall heat transferred at the condensing chamber and air-cooling system was investigated. For validation of experimental data, comparison with the simulation results of a 1D thermal-hydraulic analysis code, using the MARS model of the experimental facility in this study.

2. Experimental Setup

To experimentally investigate the overall heat removal capacity of air-cooling system, an Integrated Condensation Loop with Air-cooling System (ICLASS) facility was established as shown in Fig. 1.

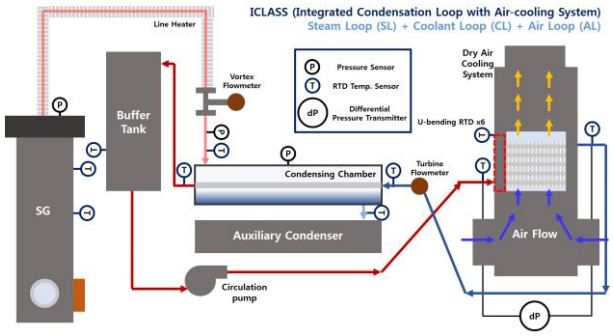

Fig. 1. Schematic diagram of ICLASS experimental facility.

2.1 Experimental Apparatus

The ICLASS facility consists of three different pressure boundaries: steam loop, coolant loop, and air loop. In the steam loop, a steam generator embedded with cartridge heaters capable of generating 18 kW heat were used for steam supply. Flow rate of the steam can be regulated by either controlling the valve at outlet of steam generator or power level of the heaters. 4 kW line heater was installed at the pipes from steam generator to the condensing chamber to prevent any early condensation. The condensing chamber is a shell and tube type heat exchanger with inner diameter of 0.1 m and contains a condensing tube with 0.0254 m in diameter and 1.0 m long. In the coolant loop, the latent heat transferred by steam condensation is carried by water and flows into one-through through 5×5 fin tube bundle which is in air flow channel. Fin tube bundle is in staggered alignment. Total heat exchanging length of the fin tube bundle is 12.5 m. Air flow cools down the hot water and send it back to the inlet of the condensing chamber. In the air loop, mechanically driven fan capable of generating 5,000 m^3/hr air flow sucks in the environmental air into the 0.5×0.5 m^2 flow channel with

1.5 m length. Every component of the ICLASS facility was insulated to minimize the heat loss.

2.2 Data Reduction

To investigate overall heat removal rate by steam condensation and air convection, four resistance temperature detectors (RTDs) were installed at the inlet and outlet of the condensing chamber and the fin tube bundle. Flow rate of the water coolant was measured by turbine flowmeter at the inlet of the condensing chamber. Then, the overall heat transfer rate at the condensing chamber (cc) and dry air-cooling system (DACS) were calculated using Eq. (1) and (2).

$$\dot{Q}_{cond} = \dot{m}_{coolant} c_p (T_{cc,out} - T_{cc,in}) \quad (1)$$

$$\dot{Q}_{air} = \dot{m}_{coolant} c_p (T_{DACS,in} - T_{DACS,out}) \quad (2)$$

Here, $\dot{Q}$, $\dot{m}_{coolant}$, c_p, and T represent overall heat transfer rate, mass flow rate, specific heat, and temperature of the coolant, respectively. When all the temperature measurement data reached steady state, data were recorded for 5 min. Averaged values of recorded data were used to calculate the overall heat transfer rate by condensation and air-cooling.

2.3 Test Matrix

Experiments were conducted by varying steam mass flow rate, water flow rate, and air inlet temperature. It should be noted that, at the current state of the ICLASS facility, air inlet temperature and flow rate could not be controlled. Thus, the air inlet temperature was altered depending on the weather and flow rate of air was maintained as 5,000 m^3/hr throughout the experiments. In addition, the steam was maintained superheated at 111°C by operating the line heater. Test matrix for this study is summarized in Table 1.

Table I: Test matrix for the experiments

Case	Steam Mass Flow Rate [kg/s]	Water Flow Rate [LPM]	Air Inlet Temperature [°C]
1	0.0038	25.8	-2
2	0.005	25.8	-2
3	0.0061	25.8	-2
4	0.0044	12.6	-4
5	0.0044	19.3	-4
6	0.0044	25.8	-4
7	0.0058	25.8	1
8	0.0058	25.8	4
9	0.0058	25.8	13

3. MARS Modeling of ICLASS Facility

Figure 2 shows a schematic view of the ICLASS modeling and nodalization. The condensing chamber and the air-cooling system of the ICLASS are modeled as two hydrodynamic components of the shell and tube sides and one heat structure. For condensing chamber, each part of the hydrodynamic component is modeled as a pipe component having 10 volumes and 9 junctions with a total length of 1 m. In case of the air-cooling system, the heat is exchanged only at the portion where fin tube bundle exists. Thus, the hydrodynamic components of the air-cooling system are modeled as a pipe component having 5 volumes and 4 junctions with a total length of 0.3 m. Remaining length of the air flow channel was modeled by attaching single volumes before and after the hydrodynamic component. The hot steam is injected into the shell side of the condensing chamber at constant mass flow rate, and the water flows in closed circuit of tube. As the steam gradually condenses, the coolant is heated up and the hot coolant is then cooled by the air flow.

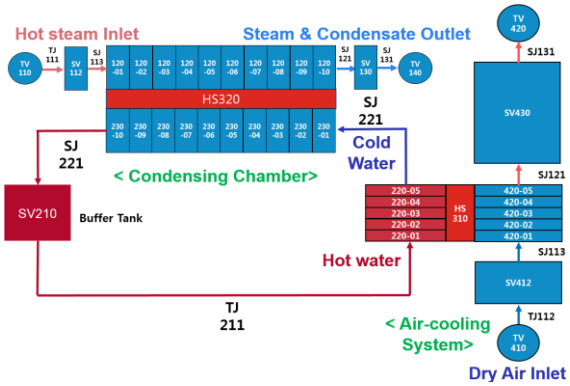

Fig. 2. MARS modeling and nodalization of the ICLASS facility.

4. Results and Discussions

4.1 Steam Mass Flow Rate Effect

Figure 3 shows the change of overall heat transfer rate at the condensing chamber and air-cooling system along with variation of steam mass flow rate. It shows increase in both by condensation and air-cooling with increasing steam mass flow. The air-cooling system well responses to the change in condensation heat transfer rate and rejects equivalent heat to the environmental air. Nevertheless, it should be noted that as the amount of steam entering the condensing chamber increases, the rate of heat carried into the chamber also increases. As the steam at the inlet of condensing chamber was kept superheated, heat input rate at the condensing chamber was calculated using Eq. (3). By comparing the ratio of the rejected heat to heat input rate, we can notice that the heat removal efficiency decreases with the increase of steam mass flow rate. Table II summarizes the temperature change of the water for cases 1, 2, and 3. Increase in steam mass flow results in increase of coolant bulk temperature inside the condensing tube meaning that more steam condensation had occurred. The increase in coolant bulk temperature inside the condensing tube results in less subcooling of the

condensing surface. Thus, the overall efficiency of heat removal decreases.

$$\dot{Q}_{in} = \dot{m}_{steam} h_{in} \quad (3)$$

Here, h_{in} is the specific enthalpy of the superheated steam at the inlet of the condensing chamber.

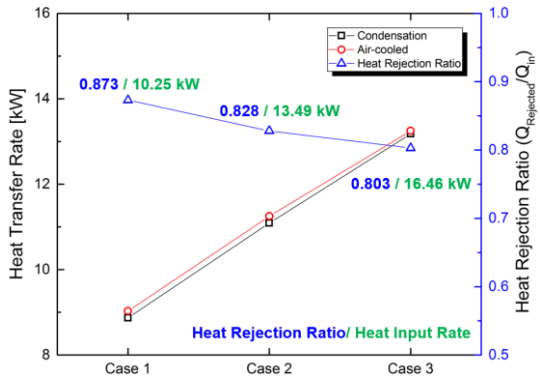

Fig. 2. Steam mass flow effect on overall heat removal efficiency.

Table II: The change of water temperature along with steam mass flow rate

Case	Heat Input Rate [kW]	Water Inlet Temp. [°C]	Water Outlet Temp. [°C]	ΔT [°C]	Rejected Heat [kW]
1	10.25	34.26	39.23	4.97	8.95
2	13.49	41.23	47.46	6.23	11.17
3	16.46	49.39	56.82	7.43	13.22

4.2 Water Flow Rate Effect

Figure 3 shows the change of overall heat transfer rate with variation of the water flow rate. It simply shows the increase in overall heat transfer rate and heat rejection ratio as the water flow rate increases. This is due to the increase in forced convective heat transfer inside the condensing tube. Larger surface sub-cooling can be achieved as water flow rate increases. As shown in Table III, bulk water temperature for case 4, 5, and 6 are similar but shows decrease in temperature difference between inlet and outlet as coolant flow rate increases.

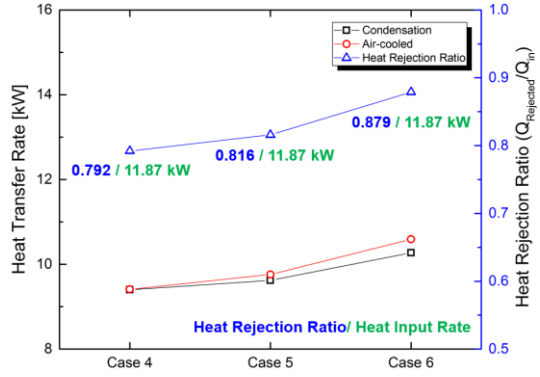

Fig. 3. Water flow rate effect on overall heat removal efficiency.

Table III: The change of water temperature along with water flow rate

Case	Heat Input Rate [kW]	Coolant Inlet Temp. [°C]	Coolant Outlet Temp. [°C]	ΔT [°C]	Rejected Heat [kW]
4	11.87	32.08	42.86	10.78	9.41
5	11.87	33.96	41.15	7.19	9.69
6	11.87	37.14	42.9	5.76	10.43

4.3 Air Inlet Temperature Effect

The effect of air inlet temperature on overall heat transfer rate and heat rejection ratio is shown in Fig. 4. Decreasing trends are observed for both parameters. In addition, when the air temperature is 13°C (Case 9), the water bulk temperature reaches over 60°C showing a large jump compared to the results of case 7 and 8 as shown in Table IV. These results indicate that the environment air temperature directly affects the heat transfer efficiency like in the results for the coolant flow rates. However, unlike the water flow rate, environment temperature cannot be controlled and may dramatically change over 30°C in one day considering the weather of desert. Thus, heat transfer efficiency of the suggested air-cooling system could be dominantly affected by the environment temperature.

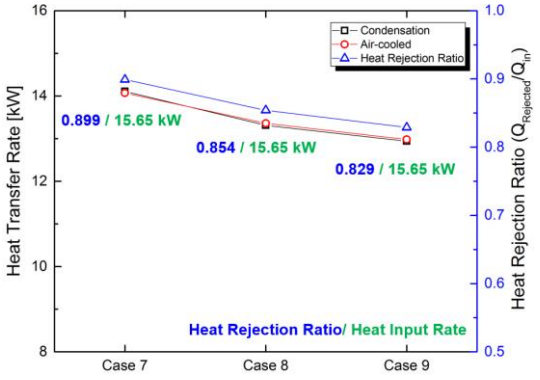

Fig. 4. Air inlet temperature effect on overall heat removal efficiency.

Table IV: The change of water temperature along with air inlet temperature

Case	Heat Input Rate [kW]	Water Inlet Temp. [°C]	Water Outlet Temp. [°C]	ΔT [°C]	Rejected Heat [kW]
7	15.65	53.57	61.58	8.01	14.07
8	15.65	54.23	61.75	7.52	13.36
9	15.65	61.16	68.56	7.40	12.98

4.4 MARS Simulation of the ICLASS Facility

Figure 5 shows a comparison of heat transfer rate by steam condensation and air-cooling between experiments and MARS simulation. The results show large difference in the amount of heat transferred. Nevertheless, MARS simulation results follow similar trends with the experimental data. This discrepancy can be expected from the condensation model in the MARS code. The MARS code adopts Nusselt's theoretical model [5] and Shah's correlation in case of external surface condensation. The Nusselt's model was derived for purely laminar film condensation and do not consider vapor velocity effect. The Shah's correlation can be used only if when the vapor quality is lower than a unity.

The difference could be induced from two contradictions with Nusselt's assumption. First, partially dropwise mode of condensation was observed during the experiments. Generally, dropwise mode of condensation shows much higher heat transfer capability over the filmwise. Secondly, the experiments were carried out with different steam mass flow rate, i.e. varying steam velocity. Strong effect of steam velocity on the overall heat transfer was observed during the experiments while Nusselt's model do not consider the steam velocity.

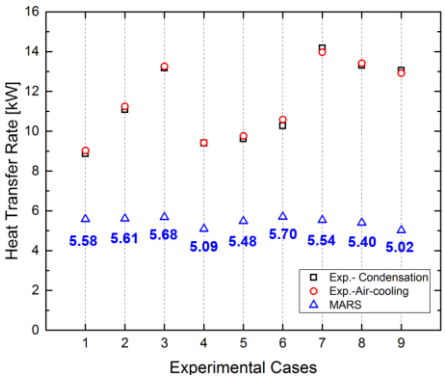

Fig. 5. Comparison of heat transfer rate between experiment and MARS simulation.

5. Conclusions

In this study, heat removal efficiency of the air-cooling system as a final heat sink of the ATOM system was investigated. Integrated condensation loop with air-cooling system (ICLASS) experimental facility was established. Heat transferred by condensation and air-cooling was compared by varying thermal-hydraulic conditions, i.e. steam mass flow rate, water flow rate, and air inlet temperature. The experimental results were compared with the MARS simulation of ICLASS facility. Major findings are as follows:

- During the investigated cases of experiments, air-cooling system showed excellent response to the change of thermal-hydraulic conditions. Heat rejected by the condensation was equally removed by means of convective heat transfer of air flow without any significant increase in coolant temperature.
- As more steam flows into the condensing chamber, the amount of heat transferred was significantly increased. However, the fraction of heat removed from the initial heat input rate showed decreasing trend. This implies that heat removal efficiency of the system deteriorates with an increase in steam mass flow rate.
- The change of heat transfer rate with water flow rate and air inlet temperature was quite straightforward. Amount of heat transferred increased with faster water flow and lower air temperature.
- The MARS simulation of the ICLASS facility showed large discrepancy with the experimental data. This difference could be caused by the partially dropwise mode of condensation and steam velocity which are not considered in the Nusselt's theoretical model in MARS code.

For future study, experimental results will be validated using theoretical or empirical models that consider the steam velocity. In addition, investigation on condensation model in MARS code will be carried out to resolve significant underestimation of condensation heat transfer.

Acknowledgement

This research was supported by the National Research Foundation of Korea (NRF), funded by the Ministry of Science, ICT, and Future Planning, Republic of Korea (No. NRF-2016R1A5A1013919).

REFERENCES

[1] D. T. Ingersoll, Z. J. Houghton, R. Bromm, and C. Desportes, Nuscale small modular reactor for Co-generation of electricity and water," Desalination, Vol. 340, pp. 84-93, 2014.
[2] J. Lee, J. I. Lee, H. J. Yoon, and J. E. Cha, Supercritical carbon dioxide turbomachinery design for water-cooled small modular reactor application, Nuclear Engineering and Design, Vol. 270, pp. 76-89, 2014.
[3] A. A. E. Abdelhameed, H. ur Rehman, and Y. Kim, A Physics Study for Passively-Autonomous Daily Load-Follow Operation in Soluble-Boron-Free SMR, Proceedings of The International Congress on Advances in Nuclear Power Plants (ICAPP) 2017, Fukui and Kyoto, Japan, April 24-28, 2017.
[4] J. A. Heyns, Performance characteristics of an air-cooled steam condenser incorporating a hybrid dephlegmator, Master Thesis, Department of Mechanical Engineering, University of Sellenbosch, 2008.
[5] W. Nusslet, Die Oberflachenkondensation des Wasserdampfes, Z. Ver. D-Ing, Vol. 60, pp. 541-546, 1916.